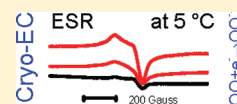


# First Direct In Situ EPR Spectroelectrochemical Evidence of the Superoxide Anion Radical

A. Petr,\* V. Kataev, and B. Büchner

Leibniz Institute for Solid State and Materials Research IFW Dresden, PF 270116, D-01171 Dresden, Germany

**ABSTRACT:** For the first time, the superoxide anion radical was formed by electrochemical reduction of oxygen and detected in situ by EPR spectroscopy without changing the temperature. The spin susceptibilities of solid superoxide solutions were measured between 280 and 4 K showing Curie behavior. The EPR results were explained in the frame of an ion association and support the formation of a loose ion pair between the superoxide anion radical and the potassium crown ether complex. An alternative explanation for the large EPR line width of the superoxide anion radical at higher temperatures is given.



## 1. INTRODUCTION

The superoxide anion radical plays an important role in the living cell, in organic and inorganic chemistry and in catalysis.<sup>1,2</sup> There are a huge number of papers which deal with the detection of superoxide anion radicals ( $\text{OO}^{\bullet-}$ ). The direct detection by EPR spectroscopy is only possible if the  $\text{OO}^{\bullet-}$  is located in a lattice or bound at a solid surface. In liquids, the detection of  $\text{OO}^{\bullet-}$  is only possible after a reaction with a second compound. Usually nitrones were used for this purpose. These nitrones are well-known as spin traps.<sup>2</sup> The result of the trap reaction is the so-called spin adduct. That means a new covalent bond between the  $\text{OO}^{\bullet-}$  and the spin trap is formed and the spin adduct is detected by EPR spectroscopy and not the  $\text{OO}^{\bullet-}$ . This method is often not unequivocal.<sup>3</sup> It is known that nitrones are susceptible to a nucleophilic addition of water especially in alkaline media.<sup>4–8</sup> The following oxidation by mild oxidants, e.g., small amounts of oxygen, will produce the same compound as formed in the case of trapping a hydroxyl radical.

In alkaline media which contain hydrogen peroxide, the perhydroxyl anion is formed. This anion is even a stronger nucleophile than water or the hydroxyl anion. Here, the nucleophilic addition of the perhydroxyl anion and subsequent oxidation will form the superoxide spin adduct which is then not a proof for  $\text{OO}^{\bullet-}$  but an artifact.

The electrochemical production of  $\text{OO}^{\bullet-}$  is quite common. However, here small amounts of water will lead to a protonation of the  $\text{OO}^{\bullet-}$  and subsequently to a formation of hydrogen peroxide.<sup>9–12</sup>

Therefore, a direct proof using the magnetic property of the  $\text{OO}^{\bullet-}$  would be very desirable. However, why is the direct detection of the  $\text{OO}^{\bullet-}$  by EPR spectroscopy so difficult?

In the free  $\text{OO}^{\bullet-}$ , the lowest energy state has a 2-fold orbital degeneracy. Therefore, we have to not only consider the spin magnetic moment but also an orbital magnetic moment which couples with the spin according to Hund's rule. It was shown by Benett et al.<sup>13</sup> that this coupling leads to a very strong dependence of the  $g$ -factor of the  $\text{OO}^{\bullet-}$  ion on the orientation in the magnetic field. If the O–O axis is oriented parallel to the external field, the  $g$ -factor should be  $g_{\parallel} = 4$  and for perpendicular

orientation  $g_{\perp} = 0$ .<sup>13</sup> In the liquid state of low viscosity, the rotational correlation time is usually short enough for averaging the  $g$  anisotropy of common organic radicals. However, in the case of the huge  $g$  anisotropy of the  $\text{OO}^{\bullet-}$  radical, this motion is too slow for averaging and leads to a very fast transverse relaxation. Therefore, it results in an extremely broad spectrum and no conventional EPR spectrometer can measure it with a reasonable signal-to-noise ratio. The  $\text{OO}^{\bullet-}$  can only be detected when the orbital degeneracy is removed by reduction of the local symmetry. Then, the  $g$ -factor is around 2.<sup>14</sup> This can be achieved by adsorption at a surface<sup>15</sup> or by distorting the symmetry in a crystal field in the solid state or in other words the association with ions or solvent molecules in frozen solutions. This is the reason for the strong dependence of the EPR spectra on the surrounding matrix.<sup>16</sup>

To our knowledge, there is only one report for the detection of the  $\text{OO}^{\bullet-}$  in the liquid state close to room temperature.<sup>17</sup> Here, the EPR susceptibility was measured in nitrile solutions far above the melting point of the solvent and the EPR susceptibility did not obey the Curie law. Unfortunately, the authors did not mention how they determined the EPR intensity. It might be that the large width of the measured spectra has influenced that finding. In the liquid phase, the intensity was strongly reduced and only the  $g_{\perp}$  part of the powder spectrum of the  $\text{OO}^{\bullet-}$  could be measured which is explained by anisotropic relaxation. However, that was the only report for a detection of  $\text{OO}^{\bullet-}$  solution above 200 K. Usually, it is reported that the EPR signal of  $\text{OO}^{\bullet-}$  disappears above 200 K.<sup>18</sup>

The present article shows that the use of appropriate counterions for the  $\text{OO}^{\bullet-}$  changes the temperature dependence of the EPR intensity significantly. This might be a new promising way for the direct detection of  $\text{OO}^{\bullet-}$ . This way will circumvent artifacts as they can happen using spin traps and will allow the detection under conditions where the spin traps are not stable. Furthermore, it is shown for the first time that the  $\text{OO}^{\bullet-}$  can be

Received: July 11, 2011

Revised: September 16, 2011

Published: September 16, 2011

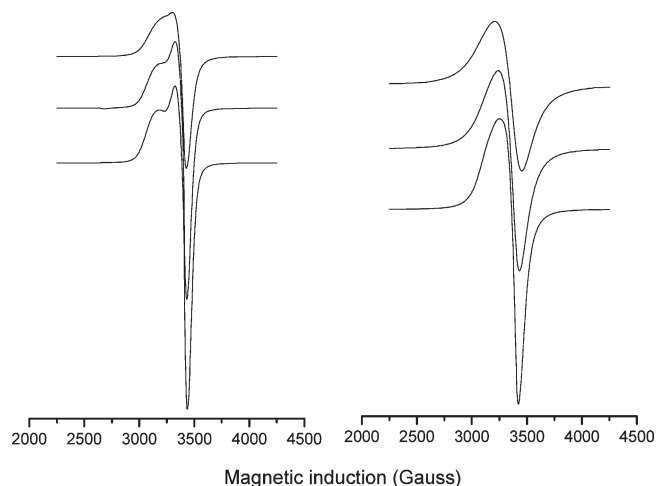


**Figure 1.** EPR spectra of  $\text{OO}^{\bullet-}$ . Left side at 4, 77, and 150 K (from bottom to top). Right side at 200, 250, and 280 K (from bottom to top).

electrochemically formed in a cavity of an EPR spectrometer in frozen DMSO and directly detected by EPR spectroscopy.

## 2. EXPERIMENTAL SECTION

**2.1. Substances and Solutions.** 2,2-Diphenyl-1-picryl-hydrazyl (DPPH), dimethylsulfoxide (DMSO) with a maximum water content of 0.005%, potassium superoxide, and the crown ether 18-crown-6 (>99.5%) were purchased from Aldrich and used as received. Tetramethylammonium tetrafluoroborate was purchased from Fluka and dried for 10 h at 80 °C and a pressure of 0.0001 mbar.

For the preparation of the solutions, an excess of potassium superoxide together with the crown ether and the DMSO were given in a mortar and were ground under nitrogen atmosphere until a yellow suspension was obtained. Afterward, the solutions were poured through a 0.2  $\mu\text{m}$  PTFE syringe filter directly into the EPR tube or flat cell. The concentration of the 18-crown-6 was 150 mM. The concentration of K was 80 mM and was determined by ICP-OES (IRIS Intrepid II XUV, Thermo Fisher Scientific). For the electrochemical investigations, the solutions mentioned above were mixed 1:1 with a 0.1 M solution of tetramethylammonium tetrafluoroborate in DMSO.

**2.2. Equipment.** EPR spectroscopy was done with an X-band spectrometer EMX (Bruker). The temperature dependent measurements were done with an  $\text{H}_{103}$  cavity equipped with a gas flow cryostat and a temperature controller ITC 503 (Oxford Instruments). A single crystal of ruby was mounted inside the cavity to have a measure for the quality factor of the cavity. For spin number determination, the double integrated signals of the samples were compared with the double integrated signal of a 5.4 mM DPPH solution in DMSO. The measurements with the flat cell were done with an  $\text{H}_{102}$  cavity equipped with a home-made temperature unit, which enables the flat part of the flat cell to be cooled down to 278 K.

**2.3. Cell Design.** For measurements above and slightly below the melting point of DMSO and for the electrochemical investigations, a flat cell made from quartz glass (QGT Quarzglas-technik, Bad Harzburg) was used. The central part of this flat cell was 0.7 mm thick. The arrangement of the electrodes was the same as shown in ref 19. The reference electrode was omitted.

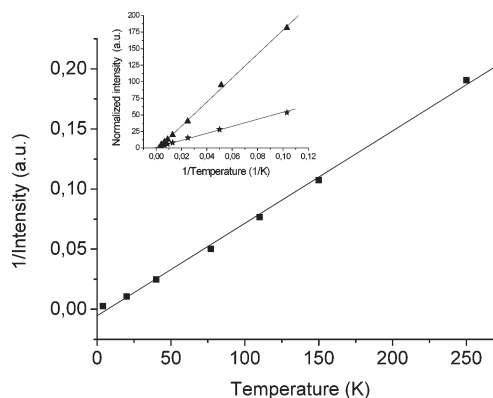


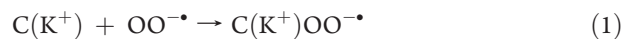
**Figure 2.** Temperature dependence of the reciprocal double integrated signal intensity for a  $\text{KO}_2$  crown ether solution in DMSO. The inset shows the double integrated signal intensity for the  $\text{KO}_2$  crown ether solution (triangles) and a 5.4 mM DPPH solution (stars) between 280 and 10 K.

The working electrode consists of a platinum mesh with a size of  $14 \times 15 \text{ mm}^2$ . We folded the mesh to get it inside the flat cell. The platinum mesh was purchased from Goodfellow and was made from a wire with 0.06 mm diameter and has 1024 meshes per  $\text{cm}^2$ . Platinum sheets of approximately  $2 \text{ cm}^2$  served as the upper and lower counter electrode.

## 3. RESULTS AND DISCUSSION

In order to detect the  $\text{OO}^{\bullet-}$  at a temperature as close as possible to the ambient temperature, we chose DMSO as solvent. If we can detect  $\text{OO}^{\bullet-}$  only a few degrees above the melting point of the solvent as it was possible in ref 17, the direct in situ detection of electrochemically generated  $\text{OO}^{\bullet-}$  should be possible, since the melting point of pure DMSO is 18 °C. DMSO is a good solvent for  $\text{OO}^{\bullet-}$ , and the stability of the  $\text{OO}^{\bullet-}$  is high enough for our investigation. The half-life at room temperature is about 100 h.<sup>20</sup> To allow a reliable double integration also for rather broad lines, we used high  $\text{OO}^{\bullet-}$  concentrations of about 18 mM. Examples of the EPR spectra at different temperatures are given in Figure 1.

For the first time, solutions of  $\text{OO}^{\bullet-}$  could be measured at 280 K with a very good signal-to-noise ratio in a single scan. This is not the case if we prepare the samples without crown ether (C). If we omit the crown ether from the sample preparation, no EPR signal of the  $\text{OO}^{\bullet-}$  is detectable at 280 K. Therefore, an association with the crown ether potassium complex, as sketched in eq 1, should be responsible for the reduction of the  $g$ -factor anisotropy.



The simulation of the powder spectrum at 4 K shows that the  $g$ -tensor is not axially symmetric and gives  $g_1 = 1.995$ ,  $g_2 = 2.014$ , and  $g_3 = 2.195$ . The simulation of the spectrum at 77 K gives  $g_1 = 2.000$ ,  $g_2 = 2.014$ , and  $g_3 = 2.185$ , indicating that already at 77 K a little averaging of the anisotropy due to the mobility of the  $\text{OO}^{\bullet-}$  occurs. The  $g$ -tensor of the spectrum obtained at 77 K is significantly different from that obtained for  $\text{OO}^{\bullet-}$  in alkaline DMSO at 77 K. In alkaline DMSO without crown ether, an axially symmetric  $g$ -tensor is found by other researchers. In ref 21,  $g_{\perp} = 2.0072$  and  $g_{\parallel} = 2.0892$  are measured. Other authors found  $g_{\perp} = 2.005$  and  $g_{\parallel} = 2.098$ .<sup>22</sup> A decrease of the symmetry is also

found when  $\text{OO}^{\bullet-}$  is adsorbed at surfaces.<sup>14</sup> This is a further hint for an interaction of  $\text{OO}^{\bullet-}$  with the potassium crown ether complex and the formation of a loose ion pair. The peak-to-peak distance at 200 K was 175 G, at 250 K 190 G, and at 280 K 240 G. The line shape is a collapsed powder pattern due to the faster reorientation of the  $\text{OO}^{\bullet-}$  at higher temperatures.

Fortunately, this increase of the line width is not as strong, still enabling a double integration of the spectrum. The temperature dependence of the double integrated signal intensity of a  $\text{OO}^{\bullet-}$  solution is shown in Figure 2. This figure clearly shows that the temperature dependence obeys Curie law. The reason for the small deviation at higher temperatures, as shown in the inset of Figure 2, might be a loss of signal intensity in the wings of the lines which is also discussed in ref 23.

In the inset of Figure 2, also the temperature dependence of a 5.4 mM solution of DPPH in DMSO is shown. Here, the lines are narrower and double integration is more precise. The linear fit of these intensities intercepts the abscissa nearly at 0, as is expected for an organic radical. The measurement of the DPPH solution with known concentration allows the determination of the spin concentration in the  $\text{KO}_2$  crown ether solution and is a good test for the equipment. Despite the small deviation at higher temperatures in the case of the  $\text{OO}^{\bullet-}$  solutions, we have no dramatic loss of the intensity with increased temperature, as is found for nitrile solutions.<sup>17</sup> That means we observe up to 280 K the whole amount of  $\text{OO}^{\bullet-}$  which the solution contains. A further striking difference between nitrile and DMSO solution is that in DMSO we were not able to detect the  $\text{OO}^{\bullet-}$  radical after the solution was molten. As soon as the solution was frozen again, we could measure an EPR signal with constant intensity. This is not the case if we leave out the crown ether. Without crown ether, we could not detect the  $\text{OO}^{\bullet-}$  radical even if we cool down to  $-10^\circ\text{C}$ .

Our explanation for the change of the shape of the EPR spectra of  $\text{OO}^{\bullet-}$  and the changed temperature behavior in crown ether containing solutions is the formation of a loose ion pair of  $\text{OO}^{\bullet-}$  and the crown ether which contains the potassium ion (see eq 1). This ion pair is formed only in the solid phase and not in the liquid phase.

Without the crown ether potassium complex, the bound  $\text{OO}^{\bullet-}$  is only formed at lower temperatures by forming a complex with the solvent. This is our explanation for the disappearance of the EPR signal above 200 K.

The good signal-to-noise ratio of the  $\text{OO}^{\bullet-}$  spectra measured in the flat cell as soon as the solution was frozen inspired us to try the direct EPR detection of electrochemically generated  $\text{OO}^{\bullet-}$  in frozen DMSO. The feasibility of electrochemical reduction or oxidation in the solid state was shown first for some frozen water containing electrolytes,<sup>24,25</sup> but there are also few reports on electrochemical investigations in frozen DMSO.<sup>26,27</sup>

These reports encouraged us to make some experiments with solid solutions of the potassium crown ether complex and dissolved oxygen. It was not a problem to reduce the oxygen in the frozen solution, but we could not detect the  $\text{OO}^{\bullet-}$  radical. We have only one explanation for this experimental result. Water is preventing the EPR detection. Already small amounts of water will immediately protonate formed  $\text{OO}^{\bullet-}$ , which leads to a very fast disproportionation, and hydrogen peroxide will be formed. A further problem is the low solubility of oxygen in DMSO. The water concentration of the driest DMSO we could buy was 2.8 mM. This concentration is too high for our experiment. We circumvented this problem by preparing solutions with an excess of  $\text{KO}_2$ . A part of the  $\text{KO}_2$  reacts with the water, forming  $\text{KOH}$ <sup>20</sup>

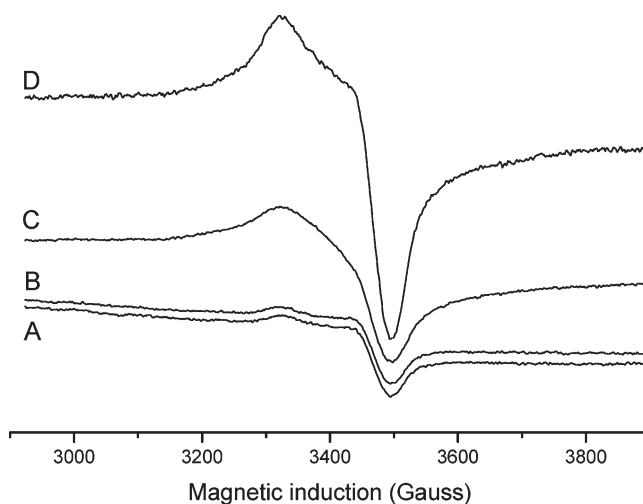
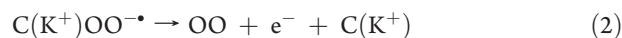


**Figure 3.** EPR spectra measured at  $5^\circ\text{C}$  with a microwave power of 32 mW in the flat cell. Modulation amplitude 60 G. Accumulated spectra from bottom to top. A: Spectrum obtained of an approximately 5 mM  $\text{OO}^{\bullet-}$  solution after oxidation with a current of  $10\ \mu\text{A}$ . B: Same solution without applying potential after 1 h. C: Same solution after applying  $-5\ \mu\text{A}$  for 1 h. D: Same solution after additionally applying about  $-3\ \mu\text{A}$  for 1.5 h.

at the end, which will not disturb our measurements. By starting with a  $\text{OO}^{\bullet-}$  solution and removing  $\text{OO}^{\bullet-}$  by electrochemical oxidation according to eq 2, we could avoid the protonation of the electrochemically formed  $\text{OO}^{\bullet-}$ .



After we had saturated the electrolyte with pure oxygen at  $15^\circ\text{C}$ , we oxidized with a current of  $10\ \mu\text{A}$  and a voltage of 0.2–0.3 V until the calculated charge for transforming the  $\text{OO}^{\bullet-}$  to  $\text{OO}$  passed. Then, we cooled the solution rapidly down to  $5^\circ\text{C}$ . As soon as the temperature was constant, we measured the EPR spectrum A in Figure 3.

To understand this spectrum, one should know that the part of the flat cell which is covered by the EPR measurement is not completely filled with the platinum mesh electrode. For the electrochemical oxidation, a part of the measured solution is too far away from the electrode. Therefore, spectrum A indicates that there was still a small amount of  $\text{OO}^{\bullet-}$  present but most of the  $\text{OO}^{\bullet-}$  was transferred to  $\text{O}_2$  which is not seen by EPR under these conditions. To be sure that the reaction of oxygen and DMSO was completed and the frozen solution was stable, we waited 1 h and measured then spectrum B in Figure 3. There is no difference between spectrum B and A. That means that no chemical reaction was changing the  $\text{OO}^{\bullet-}$  concentration. Now we started to reduce the dissolved oxygen in the frozen state with a current of  $-5\ \mu\text{A}$  by increasing the voltage between working and counter electrode from  $-0.2$  to  $-0.9$  V in a way that the current was nearly constant. After 1 h, we measured spectrum C in Figure 3. This spectrum clearly shows that we formed  $\text{OO}^{\bullet-}$  by electrochemical reduction according to eq 3.



Then, we applied a current of about  $-3\ \mu\text{A}$  for 1.5 h by increasing the voltage up to  $-2$  V and measured spectrum D in Figure 3, which has the strongest intensity compared to A, B, and C. A further increase of the applied voltage led to a decrease of



the signal intensity (not shown). This was probably due to the reduction of the  $\text{OO}^{\bullet-}$ . The  $g$ -factor measured at zero crossing with the baseline is 2.026. This is not exactly the isotropic value of the  $g$ -tensor measured in pure DMSO, but the supporting electrolyte can cause such small shift of the  $g$ -factor.

## CONCLUSIONS

The EPR line width of the  $\text{OO}^{\bullet-}$  radical can be influenced by an association of the  $\text{OO}^{\bullet-}$  with the potassium crown ether complex, forming a loose ion pair. This is confirmed by the change of the  $g$ -tensor and the temperature dependence of the EPR signal which can be measured with good signal-to-noise ratio up to 280 K. In the whole temperature range where the solution is frozen, the EPR susceptibility follows Curie law. The mobility of the oxygen, the  $\text{OO}^{\bullet-}$ , and the ions of the supporting electrolyte in frozen DMSO is high enough for an electrochemical generation of  $\text{OO}^{\bullet-}$ . The formation of the ion pair facilitates the direct EPR detection of  $\text{OO}^{\bullet-}$  at 5 °C in frozen DMSO. Our results suggest that finding another crown ether or compound which forms an ion pair also in the liquid phase will enable the direct EPR detection of  $\text{OO}^{\bullet-}$  at ambient temperature in the liquid electrolyte. This would be a big advantage for the investigation of the superoxide chemistry.

## ACKNOWLEDGMENT

We thank A. Voss for the determination of the K concentrations and R. Buckan, Ch. Scheunert, and L. Kegel for investigating the stability of the solutions by UV–vis spectroscopy. Support by the DFG through FOR 1154 is greatly acknowledged.

## REFERENCES

- (1) Sojka, Z. *Catal. Rev. Sci. Eng.* **1995**, 37, 461.
- (2) Rosen, G. M.; Britigan, B. E.; Halpern, H. J.; Pou, S. *Free Radicals—Biology and Detection by Spin Trapping*; Oxford University Press: New York, 1999.
- (3) Finkelstein, E.; Rosen, G. M.; Rauckman, E. E. *Arch. Biochem. Biophys.* **1980**, 200, 1.
- (4) Ebersson, L. *Acta Chem. Scand.* **1999**, 53, 584.
- (5) Forrester, A. R.; Hepburn, S. P. *J. Chem. Soc. C* **1971**, 701.
- (6) Bilski, P.; Reszka, K.; Bilska, M.; Chignell, C. F. *J. Am. Chem. Soc.* **1996**, 118, 1330.
- (7) Hanna, P. M.; Chamulitrat, W.; Mason, R. P. *Arch. Biochem. Biophys.* **1992**, 296, 640.
- (8) Burkitt, M. J.; Tsang, S. Y.; Tam, S. C.; Bremner, I. *Arch. Biochem. Biophys.* **1995**, 323, 63.
- (9) Sawyer, D. T.; Roberts, J. L. *J. Electroanal. Chem.* **1966**, 12, 90.
- (10) Roberts, J. L.; Morrison, M. M.; Sawyer, D. T. *J. Am. Chem. Soc.* **1978**, 100, 329.
- (11) Fee, J. A.; Hildenbrand, P. G. *FEBS Lett.* **1974**, 39, 79.
- (12) Singh, P. S.; Evans, D. H. *J. Phys. Chem. B* **2006**, 110, 637.
- (13) Bennett, J. E.; Ingram, D. J.; Symons, M. C.; George, P.; Griffith, J. S. *Philos. Mag.* **1955**, 46, 443.
- (14) Känzig, W.; Cohen, M. H. *Phys. Rev. Lett.* **1959**, 3, 509.
- (15) Howe, R. F.; Timmer, W. C. *J. Chem. Phys.* **1986**, 85, 6129.
- (16) Maricle, D. L.; Hodgson, W. G. *Anal. Chem.* **1965**, 37, 1562.
- (17) Bagchi, R. N.; Bond, A. M.; Scholz, F.; Stösser, R. *J. Am. Chem. Soc.* **1989**, 111, 8270.
- (18) Symonians, M. A.; Nalbandyan, R. M. *Biochim. Biophys. Acta* **1979**, 583, 279.
- (19) Petr, A.; Dunsch, L.; Neudeck, A. *J. Electroanal. Chem.* **1996**, 412, 153.
- (20) Gampp, H.; Lippard, S. J. *Inorg. Chem.* **1983**, 22, 357.
- (21) Hyland, K.; Auclair, C. *Biochem. Biophys. Res. Commun.* **1981**, 102, 531.
- (22) Haseloff, R. F.; Ebert, B.; Damerau, W. *Anal. Chim. Acta* **1989**, 218, 179.
- (23) Labhart, M.; Raoux, D.; Känzig, W. *Phys. Rev. B* **1979**, 20, 53.
- (24) Borgerding, A.; Brost, E.; Schmickler, W.; Dinan, T.; Stimming, U. *Ber. Bunsen-Ges. Phys. Chem.* **1990**, 94, 607.
- (25) Borkowska, Z.; Cappadonia, M.; Stimming, U. *Electrochim. Acta* **1992**, 37, 565.
- (26) Gosser, D. K.; Huang, Q. *J. Electroanal. Chem.* **1989**, 267, 333.
- (27) Diao, G.; Zhang, Z. *J. Electroanal. Chem.* **1998**, 457, 247.